IEEE Access
Multidisciplinary | Rapid Review | Open Access Journal

SPECIAL SECTION ON ADVANCED ARTIFICIAL INTELLIGENCE TECHNOLOGIES FOR SMART MANUFACTURING

Received December 30, 2020, accepted January 23, 2021, date of publication February 5, 2021, date of current version February 12, 2021.

Digital Object Identifier 10.1109/ACCESS.2021.3057415

Probabilistic Indoor Positioning and Navigation (PIPN) of Autonomous Ground Vehicle (AGV) Based on Wireless Measurements

PO TING LIN[1,2], (Member, IEEE), CHE-AN LIAO[1], AND SHU-HAO LIANG[2]

[1]Department of Mechanical Engineering, National Taiwan University of Science and Technology, Taipei 10609, Taiwan
[2]Center for Cyber-Physical System Innovation, National Taiwan University of Science and Technology, Taipei 10609, Taiwan

Corresponding author: Po Ting Lin (potinglin@mail.ntust.edu.tw)

This work was supported in part by the Ministry of Science and Technology (MOST), Taiwan under Grant MOST 108-2221-E-011-129-MY3 and Grant MOST 109-2222-E-011-008, and in part by the Center for Cyber-Physical System Innovation (CPSi), National Taiwan University of Science and Technology (NTUST), Taiwan, which is a Featured Areas Research Center in Higher Education Sprout Project of Ministry of Education (MOE), Taiwan, since 2018.

ABSTRACT Recently, Autonomous Ground Vehicles (AGV) and mobile robots have been rapidly developed in various engineering applications, such as Industry 4.0 factory and smart manufacturing. Indoor navigation was one of the most important tasks for the mobile systems as they were often designed to move from one location to another location autonomously without contacting the surrounding objects along the moving path in a usually dynamic and complex indoor environment. There were two key steps to achieve Simultaneous Localization and Mapping (SLAM). First, indoor positioning of the mobile system based on some measurements was done. The second step was to navigate itself inside the indoor map. This was a very challenging problem because there always existed uncertainties in the measurements. It was desired to estimate the positioning errors and determine a safe moving path with high reliability. This paper presented the methodologies for wireless indoor positioning and navigation of AGV with measurement uncertainties. Two kinds of AGV moving trajectories with various design parameters were simulated: a linear trajectory and a curved one. It was found that both greater number of sensors being used for wireless measurements and greater number of measurement trials for multilateration could effectively improve the accuracy of AGV positioning.

INDEX TERMS Autonomous ground vehicle (AGV), indoor positioning and navigation (IPN), Monte Carlo simulations (MCS), multilateration, wireless distance measurement.

I. INTRODUCTION

In the era of Industry 4.0, manufacturing has been moving on from industrial automations to massive needs of production customizations in smart factories. Intelligent robotics and vehicle systems have drawn great attentions and been applied for automatic customization productions [1]. One of the most attractive solutions to customized factory logistics was to use Autonomous Ground Vehicle (AGV) [2]–[5]. AGV has been used in various smart manufacturing applications with the advantages of reduced labor costs, reduced operation costs, increased reliability and productivity, and greater safety [6], [7]. However, there are still many challenges in indoor positioning and navigation (IPN) of AGVs. There were two key steps to achieve Simultaneous Localization and Mapping (SLAM) [8], [9]. First, indoor positioning of the mobile system based on some measurements was done. The second step was to navigate itself inside the indoor map. Three-dimensional measurement devices, such as stereovision and Lidar, have been greatly used for positioning of AGV [10], [11].

On the other hand, wireless indoor positioning [12] has drawn great attentions by many researchers because the sensors for wireless distance measurements are cheaper and have faster sampling rates. However, positioning based on wireless distance measurements was less accurate due to the existence of measurement uncertainties. This paper introduced the methodologies of indoor positioning based on wireless distance measurements with uncertainties. Furthermore, indoor navigation of AGV based on wireless

The associate editor coordinating the review of this manuscript and approving it for publication was Her-Terng Yau.

positioning with measurement uncertainties would be presented. The statistical performances of wireless indoor positioning were investigated to show the accuracy of AGV positioning and navigation.

II. WIRELESS INDOOR POSITIONING WITH UNCERTAINTY

A. MULTILATERATION FOR WIRELESS INDOOR POSITIONING

Assuming the wireless sensors for distance measurements are installed on a same plane, the position of the AGV, which is denoted as $\mathbf{P} = [X, Y]$, is to be estimated based on the method of multilateration [13]–[15]. Suppose there are N sensors properly installed (i.e. separated and not in a line) in the indoor workspace, the i^{th} sensor position is denoted by $\mathbf{S}_i = [S_{i,1}, S_{i,2}]$. The measurement from $\mathbf{S}_i$ to $\mathbf{P}$ is denoted as L_i and satisfies the following equation:

$$\|\mathbf{S}_i - \mathbf{P}\| = L_i \tag{1}$$

Or,

$$S_{i,1}^2 - 2S_{i,1}X + X^2 + S_{i,2}^2 - 2S_{i,2}Y + Y^2 = L_i^2 \tag{2}$$

Subtracting the Eq. (2) for the j^{th} wireless measurement from the same equation for the i^{th} measurement, the following equation is obtained:

$$A_k = B_{k,1}X + B_{k,2}Y \tag{3}$$

where

$$A_k \equiv \left(L_i^2 - S_{i,1}^2 - S_{i,2}^2\right) - \left(L_j^2 - S_{j,1}^2 - S_{j,2}^2\right) \tag{4}$$

$$B_{k,m} \equiv -2S_{i,m} + 2S_{j,m} \quad \text{for } m = 1, 2 \tag{5}$$

In Eq. (3), the index k represents each unique permutation group $\{(i, j)|i, j = 1, \ldots, N; i < j\}$. For example, when 4 sensors are used (i.e. $i, j = 1, 2, 3, 4$), the permutation groups are $\{(1, 2), (1, 3), (1, 4), (2, 3), (2, 4), (3, 4)\}$ resulting 6 different equations in Eq. (3).

At the end, the Eq. (3) can be expressed in a matrix form, as shown below:

$$\mathbf{A} = \mathbf{B}\mathbf{P} \tag{6}$$

where

$$\mathbf{A} \equiv \begin{bmatrix} A_1 \\ \vdots \\ A_k \\ \vdots \\ A_M \end{bmatrix}, \quad \mathbf{B} \equiv \begin{bmatrix} B_{1,1} & B_{1,2} \\ \vdots & \vdots \\ B_{k,1} & B_{k,2} \\ \vdots & \vdots \\ B_{M,1} & B_{M,2} \end{bmatrix} \tag{7}$$

and M is the total number of permutation groups of $\{(i, j)\}$. Since $\mathbf{B}$ is not a square matrix, the Eq. (6) cannot be solved by inverse multiplication. Least Square Approximation (LSA) could be used to find the solution with minimal squared error of the position estimation, which is given by:

$$\mathbf{P} = \left(\mathbf{B}^T\mathbf{B}\right)^{-1}\mathbf{B}^T\mathbf{A} \tag{8}$$

B. INDOOR POSITIONING WITH UNCERTAINTIES

The estimation of AGV position in Eq. (8) has the following squared error:

$$\text{Squared error} = \sum_{k=1}^{M} \left(A_k - B_{k,1}X - B_{k,2}Y\right)^2 \tag{9}$$

If each wireless measurement L_i is precise and each sensor position $\mathbf{S}_i$ is accurate, each term in Eq. (9), theoretically, could be equal to zero. However, there exists uncertainty in each measurement in practice. In this paper, the wireless measurement was assumed to be normally distributed and could be expressed as $L_i \sim N(\mu_i, \sigma_i^2)$ where $N()$ stands for normal distribution; μ_i is the mean value of the normally distributed measurement of L_i; σ_i is the standard deviation of L_i. Since L_i was randomly distributed, the estimated position of $\mathbf{P}$ was then randomly distributed. In this paper, the standard deviation of the wireless measurement was assumed fixed and independent to the distance between the sensor and the object.

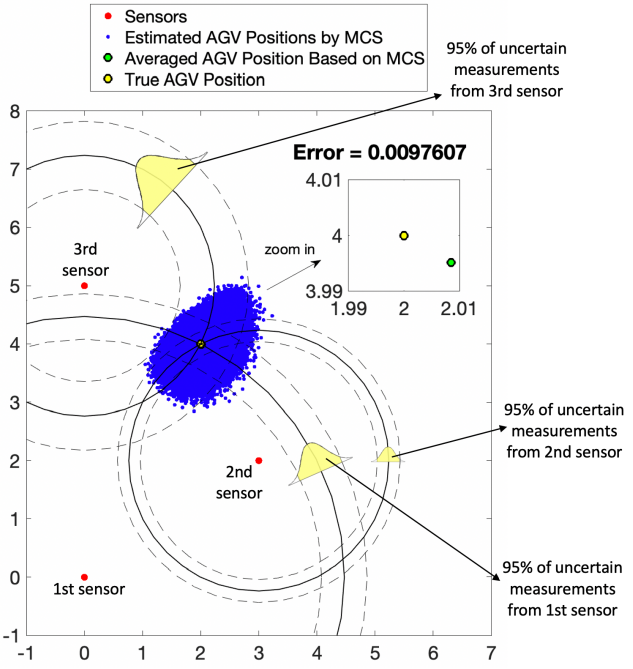

FIGURE 1. Illustration of the estimated AGV positions (blue dots; generated by 10^6 MCS) as there exist uncertainties in the measurements from three different sensors (red dots) to the true AGV position (yellow dot). Green point stands for the mean of the estimated positions obtained by MCS. Unit is meter.

Fig. 1 showed an example of the randomly distributed estimations of the AGV positions based on three sets of wireless measurements. Unit of the figure was meter. The red dots were the positions of the sensors. The positions of the first, second and third sensors were [0, 0], [3, 2], and [0, 5], respectively. The yellow dot was the true position of the AGV. The measurements from the first, second and third sensors to the AGV were assumed to be normally distributed with the standard deviations of 0.2, 0.1 and 0.3 m, respectively. We used Monte Carlo Simulations (MCS) with 10^6 trials

to estimate the AGV position with the aforementioned measurement uncertainties. The 10^6 estimated AGV positions by MCS were shown as the blue dots in Fig. 1. In the s-th MCS trial (i.e. $s = 1, \ldots, 10^6$), the i-th wireless measurement $L_i^{(s)}$ was randomly generated following the aforementioned normal distribution $N(\mu_i, \sigma_i^2)$. The s-th estimation of the AGV position $\mathbf{P}^{(s)}$ was then determined using Eq. (8).

As illustrated in Fig. 1, the random distribution of the estimated AGV positions was not normally distributed due to the geometrical relationships between the AGV position and the sensors. The mean of the 10^6 estimated AGV positions, i.e. green point in Fig. 1, was very close to the true position, i.e. yellow point. The error was less than 0.01 m. If the number of MCS was not enough, the accuracy of the averaging of AGV positions generated by MCS would be reduced. The 95%-confidence ranges of the uncertain measurements were also shown in Fig. 1. Although the uncertainty in each wireless measurement was mutually independent to each other; however, the estimation of the AGV position in Eq. (8) depended on the uncertainty from each wireless measurement. Thus, the geometrical relationship between the sensors and the AGV, as well as the uncertain level of each random wireless measurement, would affect the random distribution of the estimated AGV positions. Fig. 2 shows the accuracy of AGV positioning based on different numbers of MCS trials as each MCS was repeated for 10 times with independent random samples. From the results, it's observed that the statistical analysis of the positioning with uncertainties could be essential for the accuracy and reliability of the wireless indoor positioning of the AGV.

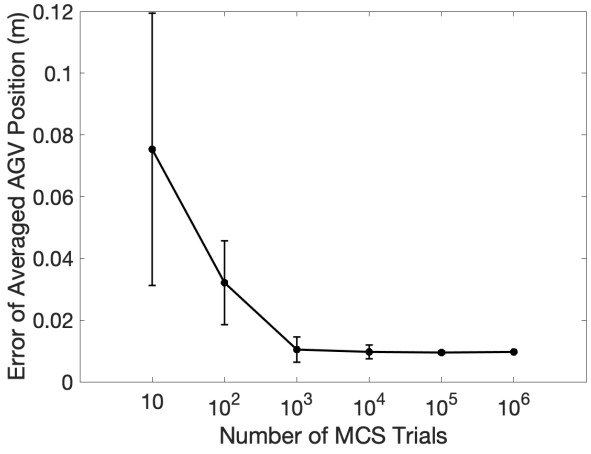

FIGURE 2. Accuracy of AGV positioning based on averaging of the estimated AGV positions generated by different numbers of MCS. Each MCS was repeated 10 times with independently generated random samples. Error bar shows the range of ±1 sigma of the 10 repeated MCS tests.

It's noted that the randomness of the estimated AGV positions was not normally distributed. At this point, the mean of the randomly distributed positions is considered as the estimated AGV position. As the uncertainty level of sensors or other components in the system increases, the randomness of the uncertainty could be more arbitrarily shaped. Statistical models such as Kernel Density Estimation (KDE) [16], [17] could be utilized to estimate the non-normally distributed AGV positions for greater accuracy of the indoor positioning. The probability of the AGV positions could then be estimated by evaluating the approximate probability density function based on the KDE models.

C. INDOOR POSITIONING OF A MOVING AGV WITH MEASUREMENT UNCERTAINTIES

The calculations in Eq. (8) assumed the AGV was stationary. Therefore, the accuracy of the AGV positioning was expected to decrease as the AGV was not stationary. The typical moving speed of an AGV for the factory is around 2 m/s. In this situation, the sampling rate of the wireless measurement needs be high enough. An illustrative example is shown in Fig. 3. An AGV was initially located at the position of $[2, 4]$ and began to move toward the position of $[-1, 2]$ with a constant speed. The duration of this movement was 1 second. Suppose the sampling rate of the wireless measurement was 1MHz, there were 10^6 sets of wireless measurements and indoor positioning based on Eq. (8) that were executed during the 1-second duration. Each estimated AGV position was illustrated by the blue points shown in Fig. 4 (a).

Since the AGV was not stationary, each set of wireless measurement was based on a different AGV position. Considering all 10^6 sets of wireless measurements for AGV positioning, as shown in Fig. 4 (a), resulted in a huge error of the estimation of the final AGV position. To resolve this issue, only the last 1000 sets of wireless measurements were considered for the estimation of the final AGV position, as shown in Fig. 4 (b). The last 1000 sets of measurements were executed within the last 1 millisecond. The movement of the AGV in the last 1 millisecond was around 0.0036 m, which was smaller than the standard deviations of the wireless measurements. Therefore, the accuracy of the estimation of the final AGV position based on consideration of the last 1000 sets of wireless measurements was 0.0156 m, which was slightly larger than the error in Fig. 1 but much more accurate than the error in Fig. 4 (a).

III. INDOOR NAVIGATION OF AGV WITH MEASUREMENT UNCERTAINTIES

A. NAVIGATION ALONG LINEAR MOVING TRAJECTORIES

In this section, a series of illustrative examples of indoor navigation of AGV were presented. The information of the sensors are given in Table 1. There were two kinds of arrangements of the wireless sensors. The first case used multilateration based on wireless measurements with sensor numbers 1∼3 as the second case used the sensor numbers 1∼4. An AGV was desired to move from a starting point $\mathbf{P}_A$: [1, 1] to an end point $\mathbf{P}_B$: [4, 4], as shown as the blue straight line in Fig. 4. Suppose there were 9 intermediate waypoints, denoted as $\mathbf{P}_1, \ldots, \mathbf{P}_9$, evenly distributed on the straight line from $\mathbf{P}_A$ to $\mathbf{P}_B$. It was assumed that the AGV was precisely

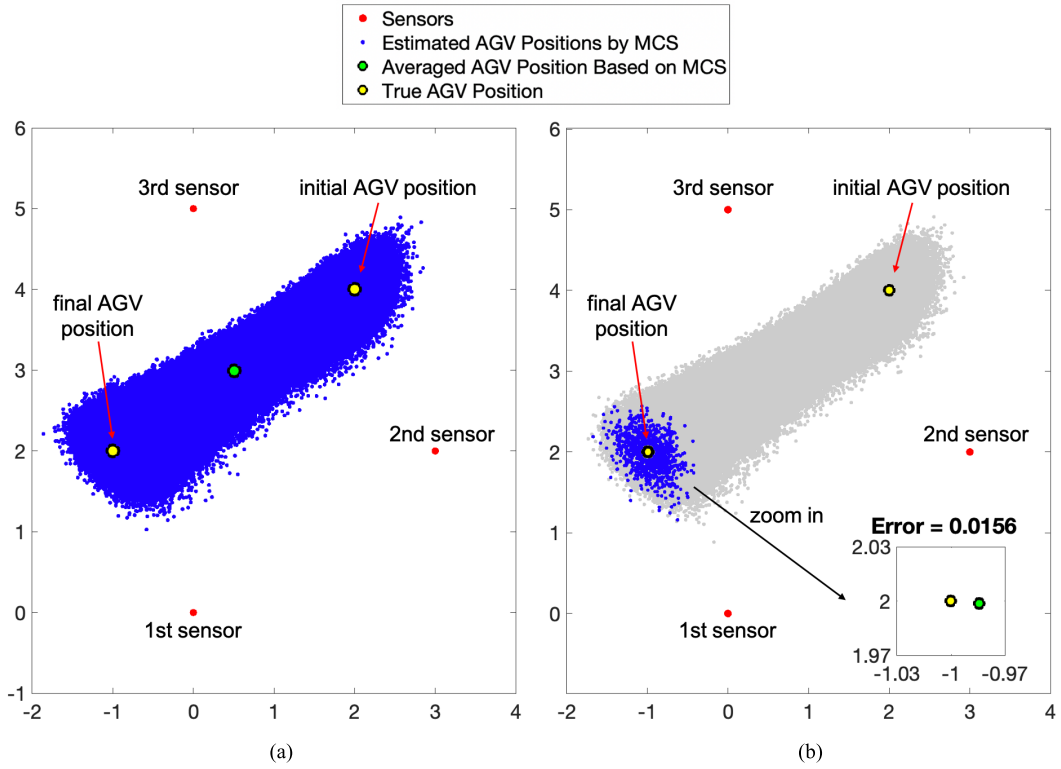

FIGURE 3. Illustration of estimating the indoor position of a moving AGV (i.e. moving from [2, 4] to [−1, 2] in 1 second) based on mean of the estimated positions determined from MCS (i.e. 10^6 samplings were made within the time): (a) taking all 10^6 points for the calculation, (b) taking the last 1000 sampling points for the calculation.

TABLE 1. Sensor information in the illustrative examples.

Sensor number	Sensor position (m)	Standard deviation of measurement (m)
1	[0, 0]	0.2
2	[3, 2]	0.1
3	[0, 5]	0.3
4	[5, 4]	0.2

placed at the starting point $\mathbf{P}_A$ at the beginning. The AGV was expected to move from $\mathbf{P}_A$ to $\mathbf{P}_B$ through each waypoint $\mathbf{P}_i$. The coordinate of each waypoint $\mathbf{P}_i$ could be computed by:

$$\mathbf{P}_i = \mathbf{P}_A + (\mathbf{P}_B - \mathbf{P}_A) \times \frac{i}{10} \tag{10}$$

It was considered that the AGV could only use the wireless measurements and multilaterations, explained in section II, to position itself. In the first example, a low number of MCS trials was considered for wireless positioning as only 10 sets of wireless measurements were considered at each waypoint, $\mathbf{P}_i$. An estimated AGV position, $\hat{\mathbf{P}}_i$, was then obtained based on averaging the 10 AGV positions from multilaterations. In Fig. 4, the true AGV positions, $\widehat{\mathbf{P}}_i$, were illustrated by the yellow points as the estimated AGV points, $\hat{\mathbf{P}}_i$, were illustrated by the green points. The cubic spline convex hull, that was illustrated by the red closed contour in Fig. 4, was used to show the range of the estimated AGV positions from multiple multilaterations. As explained in section II, the distribution of the estimated AGV positions was not normally distributed. The shape of the distribution of the estimated AGV positions varied with respect to the true AGV position and its geometrical relationship with the sensors.

At the starting point, 10 sets of multilaterations were computed using Eq. (8) with the existence of measurement uncertainties. The estimated AGV position, denoted as $\hat{\mathbf{P}}_A$, was then obtained by averaging the 10 AGV positions computed from multilaterations. The AGV was then controlled to move from $\mathbf{P}_A$ to a new position based on:

$$\widehat{\mathbf{P}}_1 = \widehat{\mathbf{P}}_A + \left(\mathbf{P}_i - \hat{\mathbf{P}}_A\right) \tag{11}$$

where $\widehat{\mathbf{P}}_A$ stands for the true position of AGV at the beginning, i.e. $\widehat{\mathbf{P}}_A = \mathbf{P}_A$ based on the assumption of precise starting point; $\widehat{\mathbf{P}}_1$ is the true AGV position at the first waypoint. It was assumed that the AGV movement, i.e. $(\mathbf{P}_i - \hat{\mathbf{P}}_A)$, was precisely done. The navigation error was only caused by the error of wireless positioning, i.e. there was error between $\hat{\mathbf{P}}_A$ and $\mathbf{P}_A$. To avoid control divergence, another run of AGV positioning based on 10 new sets of wireless measurements and multilaterations was done to obtain a new estimation of the AGV position, which was denoted as $\hat{\mathbf{P}}_1$.

At the i^{th} waypoint, the AGV was expected to move from $\widehat{\mathbf{P}}_i$ to a next waypoint, that was computed by:

$$\widehat{\mathbf{P}}_{i+1} = \widehat{\mathbf{P}}_i + \left(\mathbf{P}_{i+1} - \hat{\mathbf{P}}_i\right) \quad \text{for } i = 1, \ldots, 9 \tag{12}$$

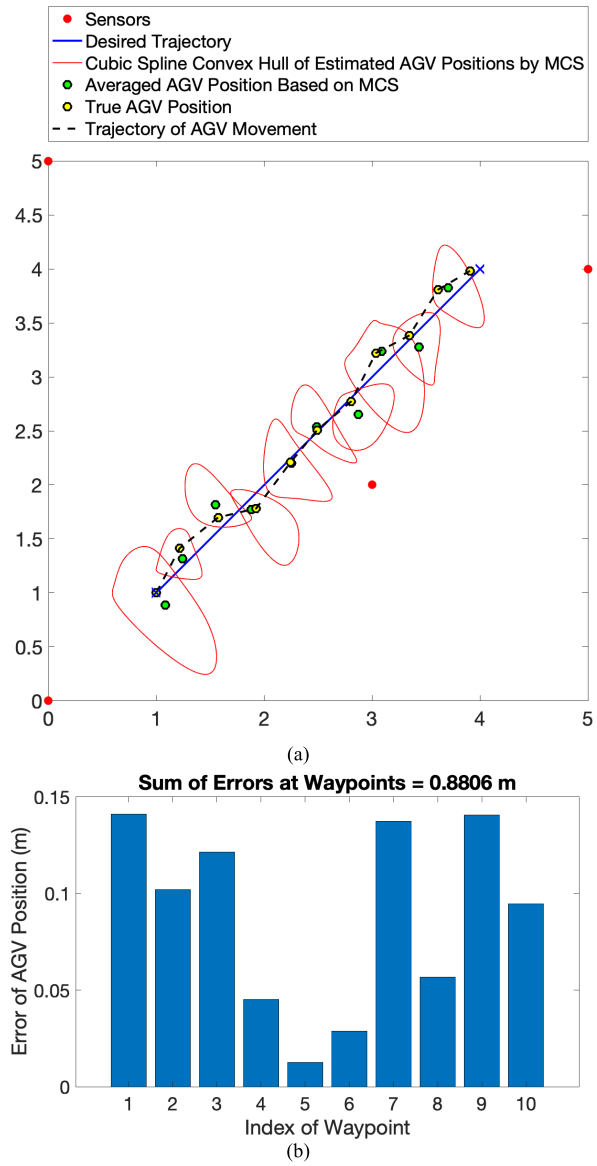

FIGURE 4. AGV navigation along a linear trajectory based on averaging of 10 sets of wireless positioning at each waypoint and 3 sensors: (a) measurement distribution and the difference between the true and estimated AGV positions at each waypoint, (b) Error of AGV position at each waypoint.

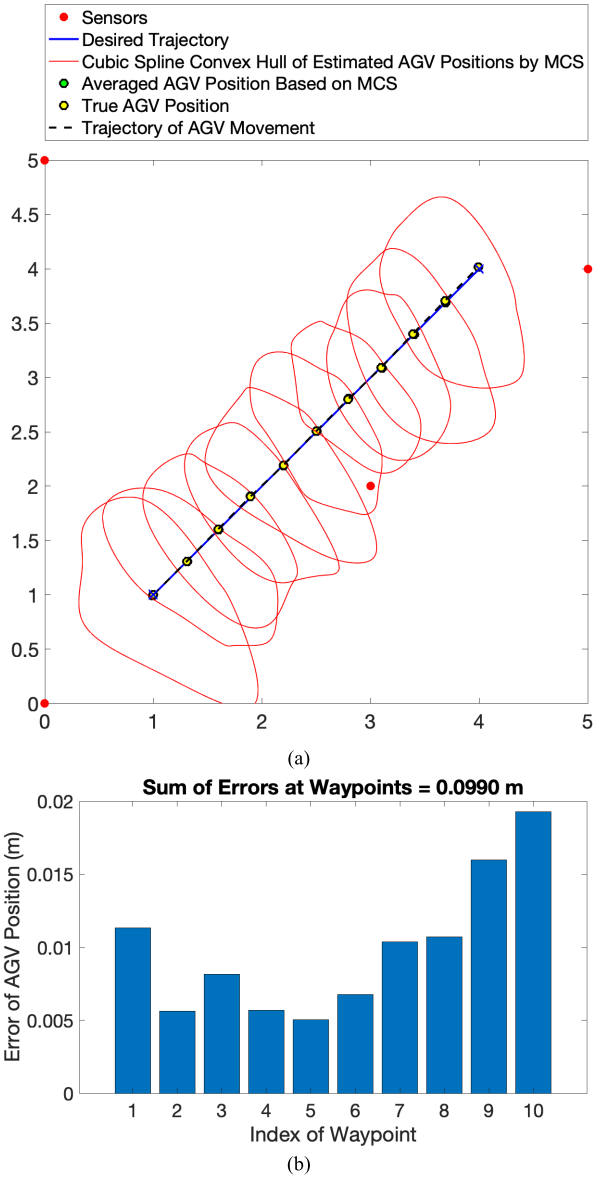

FIGURE 5. AGV navigation along a linear trajectory based on averaging of 1000 sets of wireless positioning at each waypoint and 4 sensors: (a) measurement distribution and the difference between the true and estimated AGV positions at each waypoint, (b) Error of AGV position at each waypoint.

At the end of the navigation, the final position of the AGV was $\widehat{\mathbf{P}}_{10}$. The dash line was the true trajectory of the AGV movement. It was noted that neither $\widehat{\mathbf{P}}_i$ or $\hat{\mathbf{P}}_i$ was precisely located at the desired waypoint $\mathbf{P}_i$. The true AGV position $\widehat{\mathbf{P}}_i$ was not precisely located at $\mathbf{P}_i$ because there existed measurement uncertainties in Eq. (12). The estimated AGV position $\hat{\mathbf{P}}_i$ was not accurate because only 10 sets of wireless measurements and multilaterations were used for positioning at the i^{th} waypoint. In order to quantify the accuracy of the AGV navigation, the position error at each waypoint was computed as:

$$\text{Error}_i = \left\| \widehat{\boldsymbol{P}}_i - \mathbf{P}_i \right\| \tag{13}$$

Fig. 4 (b) showed the error at each waypoint. The 10^{th} waypoint was the end point $\mathbf{P}_B$. Furthermore, the total error at every waypoint could be calculated by $\sum_i \text{Error}_i$.

The numerical simulations were repeated for 10 times. The average and standard deviation of total error of waypoints were listed in Table 2. As 10 sets of wireless measurements based on 3 sensors were used, the total error at waypoints was averagely 0.933 m. Therefore, the average error at each waypoint was around 0.093 m, which was slightly smaller than the variations of wireless measurements shown in Table 1.

In the next example, 1000 sets of wireless measurements based on 4 sensors were used at each waypoint. Fig. 5 (a)

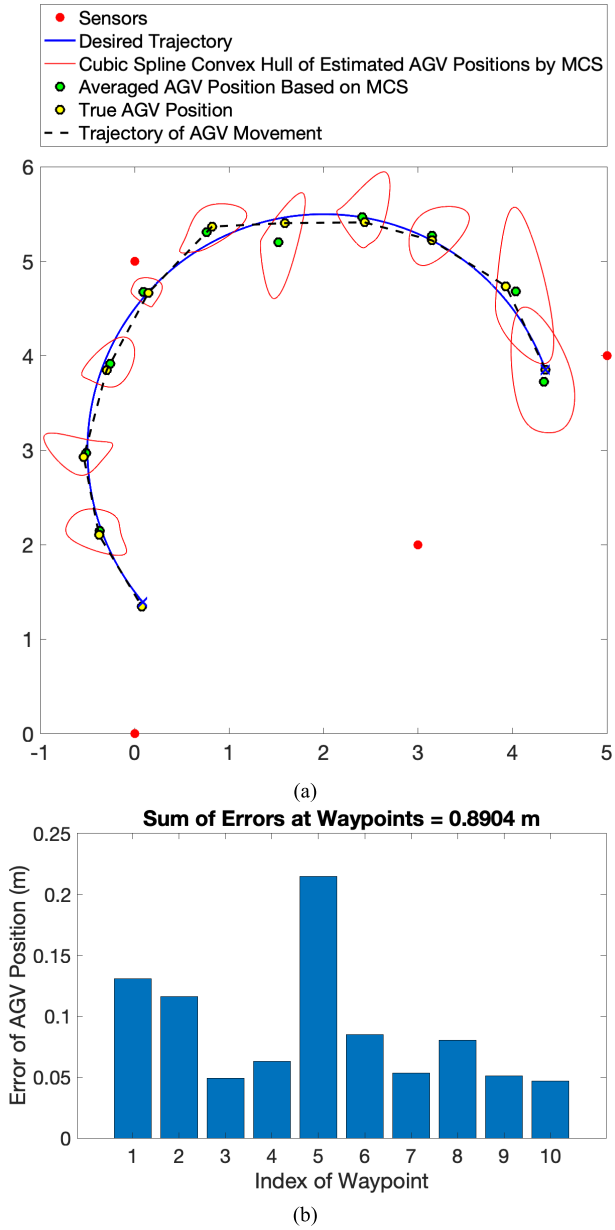

FIGURE 6. AGV navigation along a curved trajectory based on averaging of 10 sets of wireless positioning at each waypoint and 3 sensors: (a) measurement distribution and the difference between the true and estimated AGV positions at each waypoint, (b) Error of AGV position at each waypoint.

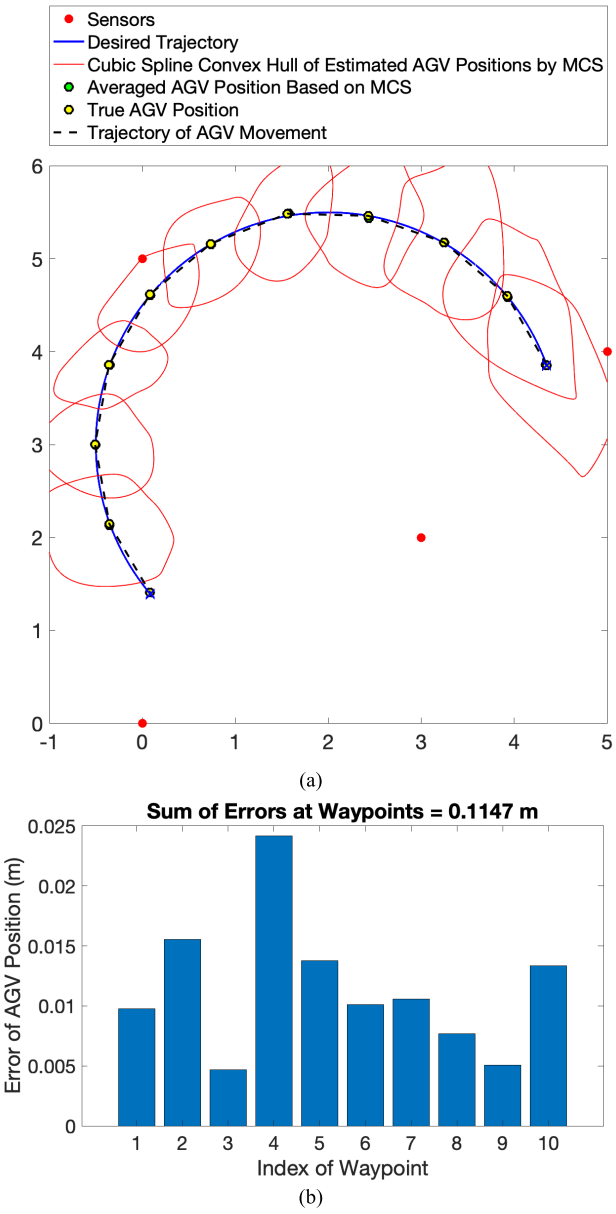

FIGURE 7. AGV navigation along a curved trajectory based on averaging of 1000 sets of wireless positioning at each waypoint and 4 sensors: (a) measurement distribution and the difference between the true and estimated AGV positions at each waypoint, (b) Error of AGV position at each waypoint.

showed that the estimated AGV positions based on 1000 sets of measurements were more precise than the one based on 10 sets of measurements. The error at each waypoint was shown in Fig. 5 (b). The total error reduced to averagely 0.113 m indicating the average error at each waypoint was only 0.011 m, which was 1 order smaller than the variations of the wireless measurements in Table 1.

From the listed results of total error of waypoints in Table 2, it was noted that more sensors were used, better accuracy indoor positioning was achieved. Furthermore, increasing the number of MCS points greatly increased the accuracy of indoor positioning.

B. NAVIGATION ALONG CURVED MOVING TRAJECTORIES

Next, the AGV was desired to move along a circular trajectory with a center at [2, 3] and a radius of 2.5 m. Fig. 6 and Fig. 7 showed an example of the curved movement. There were 9 intermediate waypoints along the curve. The blue curve was the desired trajectory. The green points were the estimated AGV positions based on multilaterations. The yellow points were the true AGV positions. The dash line was the true AGV moving trajectory. In Fig. 6 (a), 10 sets of wireless measurements based on 3 sensors were used for the positioning at each waypoint. The error at each waypoint of this case was shown in Fig. 6 (b). On the other hand,

TABLE 2. Total error of waypoints for linear movements based on 10 repeated simulations.

Number of sensors	Number of MCS trials for each positioning	Total error of waypoints
3	10	0.933±0.203
3	100	0.298±0.064
3	1000	0.136±0.016
4	10	0.802±0.134
4	100	0.260±0.022
4	1000	0.113±0.021

TABLE 3. Total error of waypoints for curved movements based on 10 repeated simulations.

Number of sensors	Number of MCS trials for each positioning	Total error of waypoints
3	10	1.083±0.222
3	100	0.321±0.067
3	1000	0.139±0.021
4	10	0.813±0.104
4	100	0.268±0.057
4	1000	0.112±0.018

Fig. 7 (a) showed one example of AGV navigation along the curved trajectory based on 1000 sets of measurements with 4 sensors at each waypoint. The error at each waypoint was shown in Fig. 7 (b). The total errors of waypoints of all tested cases were shown in Table 3. It was noted that greater number of sensors being used for wireless measurements could improve the accuracy of AGV positioning. Also, greater number of MCS trials at each waypoint improved the accuracy of AGV positioning.

IV. CONCLUSION

In this paper, the indoor positioning and navigation of Autonomous Ground Vehicle (AGV) based on wireless distance measurements with uncertainties was investigated. The distances from the AGV to multiple sensors were measured and used to estimate the AGV position based on multilateration. Since there were uncertainties in the wireless measurements, multiple sets of measurements and multilaterations were performed. The AGV position was obtained by averaging the estimated AGV positions from the Monte Carlo Simulations (MCS) of multiple wireless measurements and multilaterations. Our investigations showed that the accuracy of the AGV positioning increased as the number of MCS trials increased. Furthermore, the proposed methodologies were used for indoor navigation of AGV. In the first numerical example, the AGV was expected to move from one point to another point along a straight line. The AGV positions were determined based on the proposed wireless distance measurements and multilaterations. Although the largest standard deviation of the distance measurement was 0.3 m, the accuracy at each waypoint of the AGV was averagely 0.108 m based on 10 sets of wireless distance measurements and multilaterations (in a curved moving trajectory using 3 sensors). As the number of distance measurements and multilaterations at each way point along the desired moving trajectory increased to 1000, the accuracy at each waypoint of the AGV improved to averagely 0.014 m. The results are promising as the sensors of wireless distance measurements mostly have high sampling rates and are cheap but not accurate. Thus, these sensors are very suitable for the proposed methodologies for indoor positioning and navigation of AGV based on wireless distance measurements and multilaterations, delivering a cheap and effective solution for Simultaneous Localization and Mapping (SLAM). For example, this research group has tested the proposed method to a LiDaR (Light Detection and Ranging) sensor, which has an accuracy of ∼25 mm. With multilateration, the accuracy of indoor positioning based on the LiDaR measurements could be improved to ∼6.5 mm.

REFERENCES

[1] Z.-G. Wu, C.-Y. Lin, H.-W. Chang, and P. T. Lin, "Inline inspection with an industrial robot (IIIR) for mass-customization production line," *Sensors*, vol. 20, no. 11, p. 3008, May 2020.
[2] M. Bello, *Automated Guided Vehicles Ripe for Standardized Performance Tests*. Gaithersburg, MD, USA: National Institute of Standards and Technology, 2014.
[3] *Automatic Guided Vehicles for the Paint Shop of the Future*. Paint and Coatings Industry, Dürr, Troy, MI, USA, 2019.
[4] C. Benevides, *The Advantages and Disadvantages of Automated Guided Vehicles (AGVs)*. Bristol, CT, USA: Conveyco Technologies, 2019.
[5] Z.-Y. Chen, P.-R. Liaw, V. L. Nguyen, and P. T. Lin, "Design and manufacturing of a high-payload Mecanum-wheel ground vehicle (MWGV)," presented at the 23rd Nat. Conf. Mechanism Mach. Design (CSMMT), Tainan, Taiwan, vol. 55, 2020.
[6] M. De Ryck, M. Versteyhe, and F. Debrouwere, "Automated guided vehicle systems, state-of-the-art control algorithms and techniques," *J. Manuf. Syst.*, vol. 54, pp. 152–173, Jan. 2020.
[7] W.-Q. Zou, Q.-K. Pan, and M. F. Tasgetiren, "An effective discrete artificial bee colony algorithm for scheduling an automatic-guided-vehicle in a linear manufacturing workshop," *IEEE Access*, vol. 8, pp. 35063–35076, 2020.
[8] H. Durrant-Whyte and T. Bailey, "Simultaneous localization and mapping: Part I," *IEEE Robot. Autom. Mag.*, vol. 13, no. 2, pp. 99–110, Jun. 2006.
[9] T. Bailey and H. Durrant-Whyte, "Simultaneous localization and mapping (SLAM): Part II," *IEEE Robot. Autom. Mag.*, vol. 13, no. 3, pp. 108–117, Sep. 2006.
[10] T.-D. Vu, O. Aycard, and N. Appenrodt, "Online localization and mapping with moving object tracking in dynamic outdoor environments," in *Proc. IEEE Intell. Vehicles Symp.*, Jun. 2007, pp. 190–195.
[11] A. Kawewong, N. Tongprasit, S. Tangruamsub, and O. Hasegawa, "Online and incremental appearance-based SLAM in highly dynamic environments," *Int. J. Robot. Res.*, vol. 30, no. 1, pp. 33–55, Jan. 2011.
[12] C.-C. Chiu, J.-C. Hsu, and J.-S. Leu, "Implementation and analysis of hybrid wireless indoor positioning with iBeacon and Wi-Fi," in *Proc. 8th Int. Congr. Ultra Modern Telecommun. Control Syst. Workshops (ICUMT)*, Oct. 2016, pp. 80–84.
[13] S. Bancroft, "An algebraic solution of the GPS equations," *IEEE Trans. Aerosp. Electron. Syst.*, vols. AES–21, no. 1, pp. 56–59, Jan. 1985.
[14] P. T. Lin, P.-C. Juan, S.-P. Lin, W.-H. Lu, and Z.-G. Wu, "How end effector absolute accuracy plays a role in industry 4.0," in *Proc. 14th IEEE/ASME Int. Conf. Mech. Embedded Syst. Appl. (MESA)*, Jul. 2018, pp. 1–6.
[15] C.-A. Liao, S.-H. Liang, and P. T. Lin, "Wireless indoor positioning and navigation of AGV with measurement uncertainties," presented at the Int. Symp. Comput., Consum. Control (IS3C), Taichung, Taiwan, vol. 1341, 2020.
[16] P. T. Lin, "An efficient method of solving design optimization problems with arbitrary random distributions in gradient-based design spaces," *Struct. Multidisciplinary Optim.*, vol. 54, no. 6, pp. 1653–1670, Dec. 2016.
[17] P. T. Lin and S.-P. Lin, "An effective approach to solve design optimization problems with arbitrarily distributed uncertainties in the original design space using ensemble of Gaussian reliability analyses," *J. Mech. Des.*, vol. 138, no. 7, Jul. 2016, Art. no. 071403.

PO TING LIN (Member, IEEE) received the M.S. and Ph.D. degrees from the Department of Mechanical and Aerospace Engineering, Rutgers University, New Brunswick, USA, in 2007 and 2010, respectively.

He is currently an Associate Professor with the Department of Mechanical Engineering, National Taiwan University of Science and Technology, Taipei, Taiwan. His publications are in the following areas. His current research interests include machine vision, robotics, machine learning, reliability-based design optimization, and multidisciplinary design optimization.

Dr. Lin is the Executive Committee Member of the IEEE/ASME Mechatronic and Embedded Systems and Applications (MESA).

CHE-AN LIAO received the B.S. degree from the Department of Mechanical Engineering, National Chiao Tung University, Hsinchu, Taiwan, in 2019. He is currently pursuing the M.S. degree with the Department of Mechanical Engineering, National Taiwan University of Science and Technology, Taipei, Taiwan.

SHU-HAO LIANG received the M.S. degree from the Department of Mechanical Engineering, National Taiwan University of Science and Technology, Taipei, Taiwan, in 1999, and the Ph.D. degree from the Department of Engineering and System Science, National Tsing Hua University, Hsinchu, Taiwan, in 2005. He is currently an Assistant Professor with the Center for Cyber-Physical System Innovation, National Taiwan University of Science and Technology.